How to cite: *Angew. Chem. Int. Ed.* **2024**, *63*, e202317848
doi.org/10.1002/anie.202317848

Aromaticity

$Li_6E_5Li_6$: Tetrel Sandwich Complexes with 10-π-Electrons

Diego Inostroza[+], Luis Leyva-Parra[+], Ricardo Pino-Rios, José Solar-Encinas, Alejandro Vásquez-Espinal, Sudip Pan, Gabriel Merino,* Osvaldo Yañez,* and William Tiznado**

Abstract: When (4n +2) π-electrons are located in single planar ring, it conventionally qualifies as aromatic. According Hückel's rule, systems possessing ten π-electrons should be aromatic. Herein we report a series of D_{5h} $Li_6E_5Li_6$ sandwich structures, representing the first global minima featuring ten π-electrons E_5^{10-} ring (E = Si–Pb). However, these π-electrons localize as five π-lone-pairs rather than delocalized orbitals. The high symmetry structure achieved is a direct consequence of σ-aromaticity, particularly favored in elements from Si to Pb, resulting in a pronounced diatropic ring current flow that contributes to the enhanced stability of these systems.

[*] Dr. D. Inostroza,[+] Dr. L. Leyva-Parra,[+] Dr. J. Solar-Encinas, Prof. W. Tiznado
Centro de Química Teórica & Computacional (CQT&C), Facultad de Ciencias Exactas, Departamento de Ciencias Químicas, Universidad Andrés Bello
Avenida República 275, 8370146 Santiago de Chile (Chile)
E-mail: wtiznado@unab.cl

Dr. D. Inostroza,[+] Dr. L. Leyva-Parra,[+] Dr. J. Solar-Encinas
Doctorado en Fisicoquímica Molecular, Facultad de Ciencias Exactas, Universidad Andres Bello
Avenida República 275, 8370146 Santiago (Chile)

Dr. R. Pino-Rios, Dr. A. Vásquez-Espinal
Instituto de Estudios de la Salud, Universidad Arturo Prat
1100000 Iquique (Chile)
and
Química y Farmacia, Facultad de Ciencias de la Salud, Universidad Arturo Prat
Casilla 121, 1100000 Iquique (Chile)

Dr. S. Pan
Institute of Atomic and Molecular Physics, Jilin University
130023 Changchun (China)
E-mail: sudip@jlu.edu.cn

Prof. G. Merino
Departamento de Fisica Aplicada, Centro de Investigacion y de Estudios Avanzados Merida
Km. 6 Antigua carretera a Progreso Apdo. Postal 73, Cordemex, 97310 Mérida, Yuc. (México)
E-mail: gmerino@cinvestav.mx

Dr. O. Yañez
Núcleo de Investigación en Data Science, Facultad de Ingeniería y Negocios, Universidad de las Américas
7500000 Santiago (Chile)
E-mail: oyanez@udla.cl

[+] These authors contributed equally to this work.

Introduction

The concept of aromaticity, initially confined to organic chemistry, has undergone expansion with the integration of quantum mechanics and innovative experimental approaches.[1] A significant breakthrough occurred in 2001 with the proposal of all-metal aromaticity,[2] which has since played an invaluable role in understanding the structural and bonding characteristics of various metallic[3] and non-metallic clusters.[1b,4] Particularly, this concept has been relevant in the context of boron clusters, shedding light on their planarity and stability.[5]

In addition to π-aromaticity, it has been proposed that electrons in σ-, δ-, or φ-orbitals can also undergo delocalization, resulting in various forms of aromaticity (σ-, δ-, or φ-aromaticity). Furthermore, it has been postulated that these modes of aromaticity may coexist with similar contributions, giving rise to scenarios of multiple or conflicting aromaticity.[3,6] Despite the growing body of literature on this topic, these concepts still face scrutiny and skepticism within the scientific community.[7] Specifically, σ-aromaticity was introduced by Dewar to elucidate the anomalous magnetic properties of cyclopropane.[8] However, several groups have suggested that cyclopropane should not be classified as σ-aromatic, given its subtle stabilization energy relative to propane.[9] Nevertheless, this concept remains integral to modern chemistry, particularly in explaining why specific highly symmetrical isomers exhibit greater stability than others.[10]

In the realm of tetrel chemistry (compounds of 14 group elements), the pentagonal ring E_5^{6-} (where E = Si, Sn, and Pb) shares structural and isoelectronic similarities with the cyclopentadienyl anion (D_{5h} $C_5H_5^-$).[11] This ring has been identified in several compounds. These include Zintl phases like $Li_{12}Si_7$,[12] Na_8BaPb_6, Na_8BaSn_6, Na_8EuSn_6,[13] Li_9@x$EuSn_{6+x}$, $Li_{9-x}CaSn_{6+x}$, $Li_5Ca_7Sn_{11}$, and $Li_6Eu_5Sn_9$.[14] This E_5^{6-} moiety, comprising 26 valence electrons distributed among five σ-lone pairs, five E–E σ-bonds, and three delocalized π-bonds, satisfies Hückel's rule of aromaticity. However, the non-solubility of certain Zintl phases poses challenges in isolating these intriguing entities.[14] Some of us theoretically reported these rings in the D_{5h}–$M_7E_5^+$ (E = C–Pb and M = Li–Cs) structures.[11b,15] D_{5h} Si_5^{6-} has been recognized as a suitable building block for larger clusters like $(Li_6Si_5)_{2-5}$ systems.[16]

Numerous strategies have been proposed to stabilize aromatic hydrocarbons with ten π-electrons.[17] These strategies often involve starting with six π-electrons rings,

like benzene, and introducing four additional electrons through doping. Another approach is ensuring that π-electrons are not fully engaged in forming covalent bonds, promoting electron delocalization, and preserving or enhancing aromaticity. While these strategies apply to rings like C_nH_n (where $n=6$–8), they do not favour $n=5$. Consequently, the absence of reported structures accommodating a pentagonal tetrel ring with ten π-electrons motivates us to search for such fascinating E_5^{10-} rings that are viable to be realized.

In this study, we introduce the D_{5h} $Li_{12}E_5$ (with E = Si–Pb) systems, revealing the first global minima containing pentagons composed by tetrel atoms. These systems embody a $[Li_6]^{5+}[E_5]^{10-}[Li_6]^{5+}$ sandwich configuration, with the E_5 pentagon connected through five E–E σ-bonds and accommodating five σ- and five π-lone-pairs. Despite satisfying the Hückel 4n+2 rule for aromaticity (with ten π-electrons), these electrons avoid forming delocalized bonds. The high symmetry structure achieved is a direct consequence of σ-aromaticity, particularly favored in elements from Si to Pb, resulting in a pronounced diatropic ring current flow that contributes to the enhanced stability of these systems.

Results and Discussion

Our exploration begins by juxtaposing star-shaped clusters with D_{5h} symmetry, namely $Li_7C_5^+$ and $Li_7Si_5^+$. Despite both possessing six π-electrons, $Li_7Si_5^+$ displays also σ-aromaticity, as confirmed by induced magnetic field analysis. These results were validated by analyzing the ring current strength passing through the Si_5 or C_5 ring bonds (using AIMAll[18] at the PBE0[19]-D3(BJ)[20]/def2-TZVP[21] level). The σ- and π-ring current strengths for $Li_7C_5^+$ (2.2 and 11.0 nA/T) and $Li_7Si_5^+$ (9.8 and 11.2 nA/T) underscore the pronounced σ-aromatic character of $Li_7Si_5^+$, a quality nearly absent in $Li_7C_5^+$. This contrasts sharply with its organic counterpart, $C_5H_5^-$, where the current strengths for the σ- (1.9 nA/T) and π-components (13.1 nA/T) emphasize the dominance of the latter (Figure S1). Consequently, we hypothesize that the presence of σ-aromaticity in $Li_7Si_5^+$ and its absence in $Li_7C_5^+$ may be attributed to the position of silicon in the third period, which confers the capability to exceed the octet rule, thus providing the possibility for bonding electrons to delocalize. Under this assumption, the pentagonal rings E_5 (E = Si–Pb) emerge as strong candidates to host ten π-electrons.

Using AUTOMATON,[22] we systematically explored the potential energy surfaces (PESs), in both singlet and triplet states of $Li_{12}E_5$ combinations. Geometry optimizations were performed at the PBE0/SDDAll[23] level. The candidates were reminimized at the PBE0-D3(BJ)/def2-TZVP level. True minima were confirmed through frequency analyses at the same level. The energy of the best structures was further refined at the DLPNO-CCSD(T)[24]/CBS[25]//PBE0-D3(BJ)/def2-TZVP level.

Low-lying energy isomers for the $Li_{12}E_5$ combinations are depicted in Figures S2–S5, and the Cartesian coordinates are collected in the Supporting Information. The D_{5h} sandwich-type structure (**1**) is the most energetically favored among these. The second isomer varies based on the atom: tetrahedral structure for Si, a E_5 bent chain configuration for Ge, and dissociated structures for E = Sn and Pb. The relative energies between **1** and the closest energy isomer are 15.8 (Si), 17.2 (Ge), 12.1 (Sn), and 11.6 (Pb) kcal/mol (see Figures S2–S5).

Structure **1** comprises an E_5 ring sandwiched between two quasi-planar Li_6 moieties, adopting inverted pentagonal pyramid motifs (Figure 1). The E–E bond lengths exceed

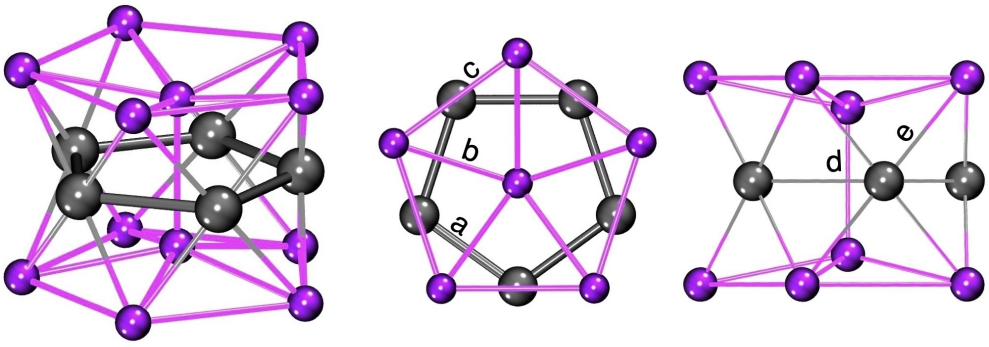

$Li_{12}E_5$ (E = Si/Ge/Sn/Pb) (D_{5h}, $^1A'_1$)

Label	Bond	Distance (in Å)
a	E-E	2.545 / 2.713 / 3.072 / 3.240
b	Li-Li	2.781 / 2.791 / 2.888 / 2.886
c	Li-Li	3.205 / 3.185 / 3.229 / 3.203
d	Li-Li	2.722 / 2.589 / 2.526 / 2.464
e	E-Li	2.496 / 2.532 / 2.721 / 2.764

Figure 1. Selected bond lengths in Å and different views of the global minimum sandwich isomer (**1**) of $Li_6E_5Li_6$.

the E–E referential single covalent bond lengths by 0.2 to 0.4 Å.[26] Among the Li atoms, three distinct Li–Li bond lengths are discernible: the peripheral Li atoms are separated by 3.2 Å, the distance between the peripheral Li and the central Li is approximately 2.8 Å, and the separation between the two central Li atoms is around 2.6 Å. The first distance is larger than the latter two, which closely approach the reference single Li–Li bond length of 2.66 Å.[26] The Li–E bond lengths of ≈2.6 Å aligns with the reference Li–E single bond length (2.49 for Si, 2.54 for Ge, 2.73 for Sn, 2.77 Å for Pb).[26]

The bond dissociation energy (BDE) for the process **1**→ E_5+2Li_6 is remarkably high (270.9 (Si), 266.9 (Ge), 260.2 (Sn), 242.4 (Pb) kcal/mol), highlighting the stability of the structure against fragmentation. To delve into the kinetic stability of **1** against isomerization, we carried out Born-Oppenheimer molecular dynamics (BOMD) simulations[27] at 400 and 500 K using the PBE0-D3/def2-SVP[21a] level, with a 0.5 fs step size over 10 ps. The consistently small median root-mean-square deviation (RMSD) values (ranging from 0.2 to 0.3 Å) across all trajectories (Figure S6) indicate minimal structural perturbations or isomerization, corroborating the kinetic stability of $Li_6E_5Li_6$.

Lithium clusters typically stabilize through multicentric bonds, such as 3c–2e or 4c–2e bonds. In contrast, our system features Li atoms that predominantly act as Li^+ ions, contributing to the electrostatic stabilization of the D_{5h}–Si_5^{10-} system. Natural population analysis indicates that each peripheral lithium atom bears a charge of approximately +0.8 *e*, while each central lithium carries a charge close to +0.3 *e*. Conversely, the E atoms bear charges around −1.7 *e* (see Table S1). This leads us to describe the complex as $[Li_6]^{4.3+}[E_5]^{8.6-}[Li_6]^{4.3+}$ or, in an idealized form, as $[Li_6]^{5+}[E_5]^{10-}[Li_6]^{5+}$.

An adaptive natural density partitioning (AdNDP)[28] analysis of **1**, compared to the D_{5h} $Li_7Si_5^+$ cluster provides further insights. $Li_7Si_5^+$ has five lone pairs (one on each Si atom), five 2c–2e peripheral Si–Si σ-bonds, and three delocalized π-bonds residing on the Si_5 ring, akin to the cyclopentadienyl anion (Figure 2a). In contrast, **1** retains the σ-bonding framework but accommodates ten π-electrons occupying the five E(p_z) orbitals as lone pairs. AdNDP analysis confirms that the E_5 pentagon in **1** is connected exclusively through five 2c–2e E–E σ-bonds, consistent with the Wiberg Bond Index (WBI) values[29] and expected distances for a single E–E bond (Table S1). Moreover, a 12c–2e multicenter bond involving the two Li_6 fragments becomes apparent, delocalizing through the center of the E_5 pentagon and corresponding to a WBI value close to 0.2 between the central Li atoms (Table S1).

The Electron Localization Function (ELF)[30] in D_{5h} $Li_{12}Si_5$ system (Figure 3b) also reveals regions associated with lone pairs and bonding electrons. In a plane 0.8 Å parallel to the E_5 ring, lone pair regions intensify while the bonding regions vanish, contrasting with $Li_7Si_5^+$ (where the plane views and the integrated density values within the basins are consistent with AdNDP analysis, Figure 3a). This aligns with the absence of π-bonds in $Li_{12}Si_5$ and emphasizes the presence of two lone pairs on each Si atom. In the bottom of Figure 3, the integrated values in the basins show populations of 1.36 *e* for the Si–Si bonds and ten basins, each with a population of 2.31 *e* (for each p_z-lobe). So, these results support that the E_5 pentagon is interconnected by ten σ-bonds, hosting ten π-electrons located as lone pairs in their respective p_z orbitals.

AdNDP indicates the presence of a delocalized 12c-2e bond involving twelve Li atoms, corresponding to the two basins detected by ELF, each with a population of 0.71 *e*. The recognition that this species is a biradicaloid by both AdNDP and ELF is noteworthy, in agreement with the fact that the stable wave function for these systems is derived from an unrestricted calculation. Furthermore, the triplet energies for **1** are higher by 15.9, 10.6, 17.8, and 18.1 kcal/mol for Si, Ge, Sn, and Pb, respectively. See computational details in the Supporting Information.

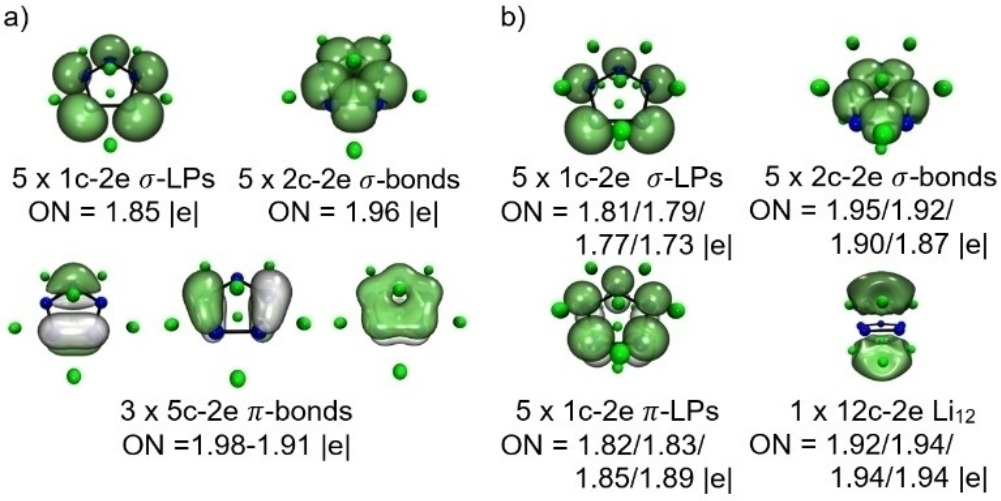

Figure 2. The AdNDP orbitals of a) $Li_7Si_5^+$ and b) $Li_6E_5Li_6$ (E = Si/Ge/Sn/Pb).

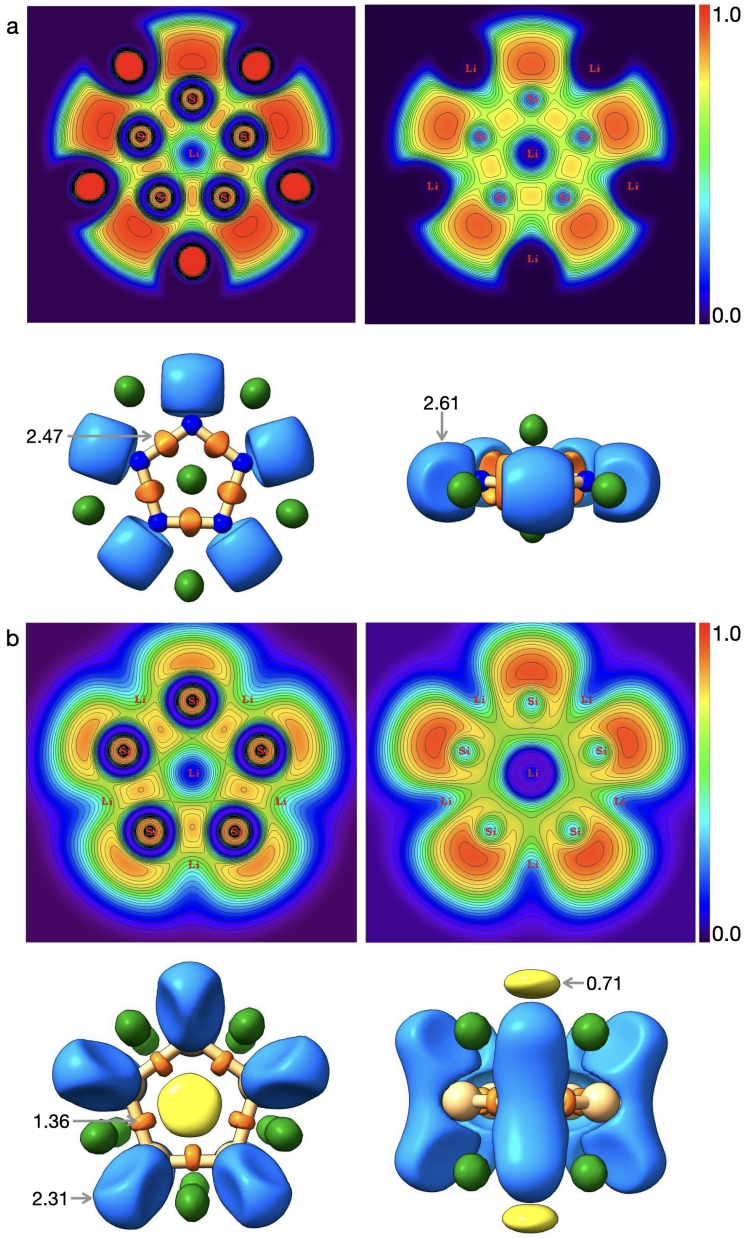

Figure 3. Electron Localization Function for two distinct systems. (a) The top panel showcases the contours in the Si_5 plane for the D_{5h}–$Li_7Si_5^+$ system, while the bottom panel reveals its corresponding isosurfaces. (b) The upper and lower panels illustrate the contours in the Si_5 plane and the isosurfaces for the D_{5h}–$Li_{12}Si_5$ system. Values correspond to integrated electron density over the corresponding basins.

So, the bond analysis shows that each tetrel atom within the E_5 pentagonal ring satisfies the octet rule, encompassing eight electrons—two from single E–E bonds and two from lone pairs. However, the ten π-electrons resist participating in covalent bonds, suggesting that the E_5 rings, despite being planar and symmetrical, lack π-aromatic character. To delve further, we explored magnetic behavior, particularly the magnetically induced current density.

Current density computations were conducted using the GIMIC program[31] at the PBE0-D3(BJ)/def2-TZVP level, with an external magnetic field perpendicular to the E_5 ring. The ring current strength was determined by integrating the ring current flow in planes perpendicular to the molecular planes. Note that the integration planes were selected to separate contributions from each fragment, as outlined in Figure 3a (with a height of 2 Å).

Let us focus on structure **1** of $Li_{12}Si_5$. Figure 4a shows an isosurface of current density modulus, illustrating distinct diatropic regions enveloping the Li_6 and Si_5 blocks. Bifurcation regions aided in defining domains associated with each molecular fragment. Figure 4b outlines the planes used to plot vector representations of current densities. These vector representations are further elucidated in Figure 4c, unveiling clockwise diatropic ring currents at the Si_5 and Li_6 planes, indicative of aromaticity. Importantly, this aromatic behavior diminishes 1 Å above the plane, signifying its σ-nature.

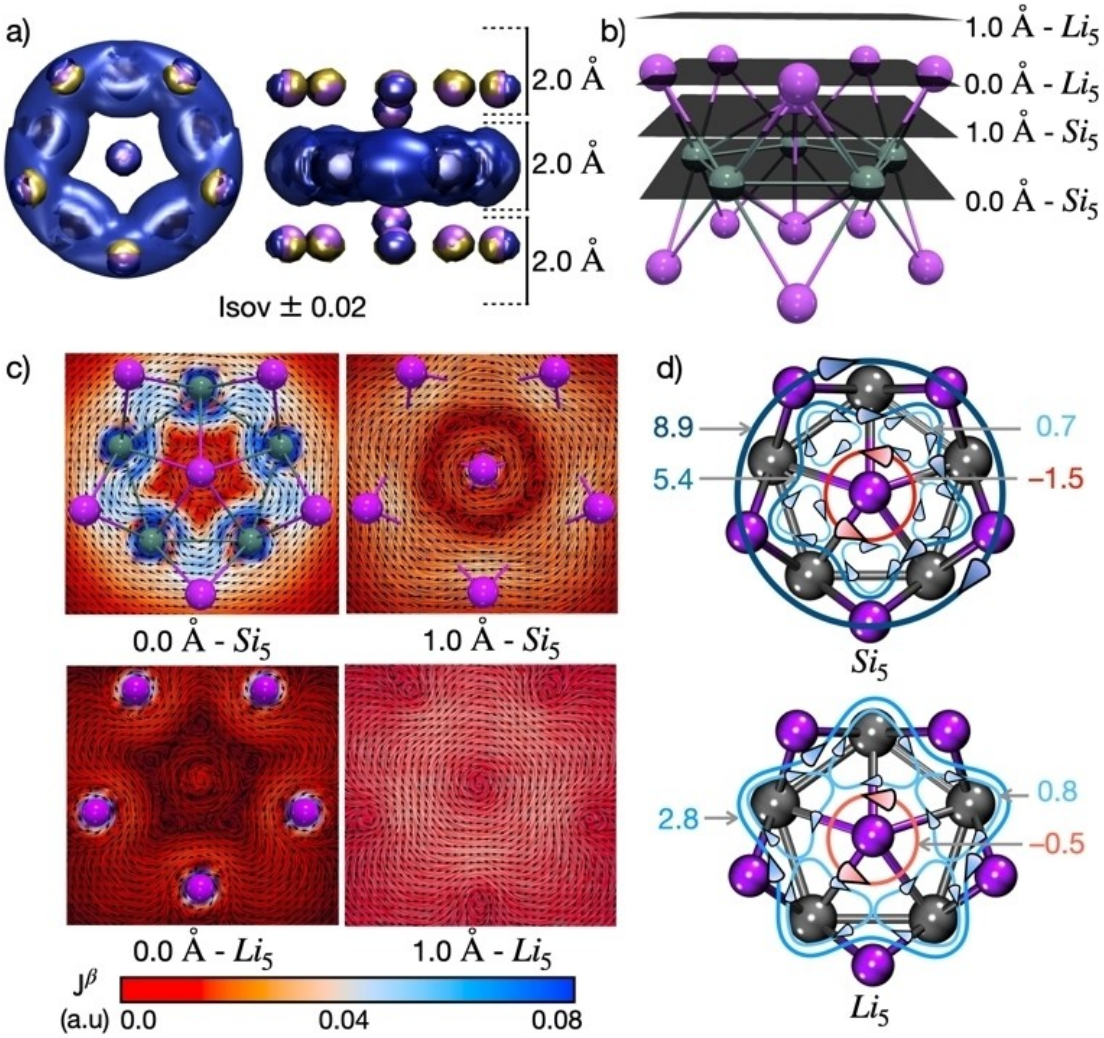

Figure 4. a) Signed modulus of the current density for **1** (E = Si, diatropic component in blue). b) Selected planes for vector plot current density. c) Vector plots of the current density. d) The identified ring current circuits in the Si_5 and Li_6 fragments with their respective RCS values in nAT^{-1}.

Figure 3d provides schematic representations of identified ring current circuits and their strengths in nA/T (see Figures S7–S9). The Si_5 ring exhibits two concentric diatropic ring currents with 8.9 and 5.4 nA/T strengths. Additionally, a paratropic ring current at the center has a strength of −1.5 nA/T. The net ring current strength is 12.8 nA/T. In contrast, the Li_6 fragment displays a weak diatropic ring current of 2.8 nA/T and a paratropic counterpart of −0.5 nA/T, resulting in a net ring current strength of 2.3 nA/T. This confirms the aromatic character of the Si_5^{10-} and Li_6^{5+} moieties, wherein the former displays strong aromaticity compared to the latter, a trend evident when compared with the net ring current strengths in C_6H_6 and $C_5H_5^-$ of 11.8 and 12.9 nA/T, respectively. Further verification of the σ-nature of the ring current in Si_5^{10-} was attained through the evaluation of σ- and π-contributions in Si_5^{10-} (13.6 and 1.1 nA/T) and Li_{12}^{10+} (1.7 nA/T) (Figure S10). A more detailed insight can be found in the supporting material.

We also explored the PES of $M_{12}E_5$ combinations, where E varies from Si to Pb, and M encompasses Na and K. In most cases, the D_{5h} form is a local minimum. An exception occurs with $K_{12}Sn_5$ and $K_{12}Pb_5$, where the symmetrical structures are transition states. Notably, the D_{5h}-$Na_{12}Sn_5$ arrangement is only 0.8 kcal/mol above the global minimum at a PBE0-D3(BJ)/def2-TZVP level (see Figure S11). These findings highlight the pivotal role of lithium.

Conclusion

We have reported the global minima for $Li_{12}E_5$ (E = Si–Pb) combination by comprehensively exploring the potential energy surface. This exploration revealed unique sandwich-type structures characterized by the presence of inverted quasi-planar pentagonal pyramidal Li_6^{5+} units as the 'bread,' encapsulating the pentagonal E_5^{10-} ring as the 'filling.' The E_5^{10-} ring accommodates ten π-electrons within the $E(p_z)$ orbitals, while the σ-electrons are distributed in five lone

pairs and five single E–E bonds. Intriguingly, although the E atoms satisfy the octet rule, our analysis of magnetic behavior reveals a strong diatropic ring current response to external magnetic fields, underlining pronounced σ-aromatic character as a key stabilizing factor.

Acknowledgements

This work was supported by the financial support of the National Agency for Research and Development (ANID) through Fondecyt projects 1211128 (W. T.), 1221019 (A. V.-E.) and 1230571 (R. P.-R.) and National Agency for Research and Development (ANID)/Scholarship Program/Becas Doctorado Nacional/2019-21190427 (D. I.) and 2020-21201177 (L. L.-P.). Scholarship Program/Becas Doctorado UNAB (J. S.-E). Powered@NLHPC: This research was partially supported by the supercomputing infrastructure of the NLHPC (ECM-02).

Conflict of Interest

The authors declare no conflict of interest.

Data Availability Statement

The data that support the findings of this study are available in the supplementary material of this article.

Keywords: Aromaticity · Bonding · Global Minimum · Sandwich · Stability · Ten π-Electrons · Tetrel Chemistry

[1] a) G. Merino, M. Solà, I. Fernández, C. Foroutan-Nejad, P. Lazzeretti, G. Frenking, H. L. Anderson, D. Sundholm, F. P. Cossío, M. A. Petrukhina, J. Wu, J. I. Wu, A. Restrepo, *Chem. Sci.* **2023**, *14*, 5569–5576; b) M. Solà, A. I. Boldyrev, M. K. Cyrañski, T. M. Krygowski, G. Merino, in *Aromaticity and antiaromaticity: concepts and applications*, John Wiley & Sons, Hoboken, **2022**; c) I. Fernández, in *Aromaticity: Modern Computational Methods and Applications*, Elsevier, Amsterdam, **2021**.

[2] X. Li, A. E. Kuznetsov, H.-F. Zhang, A. I. Boldyrev, L.-S. Wang, *Science* **2001**, *291*, 859–861.

[3] a) J. M. Mercero, A. I. Boldyrev, G. Merino, J. M. Ugalde, *Chem. Soc. Rev.* **2015**, *44*, 6519–6534; b) A. I. Boldyrev, L.-S. Wang, *Chem. Rev.* **2005**, *105*, 3716–3757.

[4] C. Liu, I. A. Popov, Z. Chen, A. I. Boldyrev, Z. M. Sun, *Chem. Eur. J.* **2018**, *24*, 14583–14597.

[5] a) A. P. Sergeeva, I. A. Popov, Z. A. Piazza, W.-L. Li, C. Romanescu, L.-S. Wang, A. I. Boldyrev, *Acc. Chem. Res.* **2014**, *47*, 1349–1358; b) A. N. Alexandrova, A. I. Boldyrev, H.-J. Zhai, L.-S. Wang, *Coord. Chem. Rev.* **2006**, *250*, 2811–2866; c) S. Pan, J. Barroso, S. Jalife, T. Heine, K. R. Asmis, G. Merino, *Acc. Chem. Res.* **2019**, *52*, 2732–2744.

[6] a) C. A. Tsipis, *Coord. Chem. Rev.* **2005**, *249*, 2740–2762; b) A. I. Boldyrev, L.-S. Wang, *Phys. Chem. Chem. Phys.* **2016**, *18*, 11589–11605.

[7] a) S. K. Ritter, *C&E News Online* **2015**, *93*, 37–38; b) R. Hoffmann, *Am. Sci.* **2015**, *103*, 1511.

[8] M. J. S. Dewar, *Bull. Soc. Chim. Belg.* **1979**, *88*, 957–967.

[9] W. Wu, B. Ma, J. I-Chia Wu, P. v. R. Schleyer, Y. Mo, *Chem. Eur. J.* **2009**, *15*, 9730–9736.

[10] I. A. Popov, A. A. Starikova, D. V. Steglenko, A. I. Boldyrev, *Chem. Eur. J.* **2018**, *24*, 292–305.

[11] a) W. Tiznado, N. Perez-Peralta, R. Islas, A. Toro-Labbe, J. M. Ugalde, G. Merino, *J. Am. Chem. Soc.* **2009**, *131*, 9426–9431; b) A. Vásquez-Espinal, K. Palacio-Rodríguez, E. Ravell, M. Orozco-Ic, J. Barroso, S. Pan, W. Tiznado, G. Merino, *Chem. Asian J.* **2018**, *13*, 1751–1755.

[12] H. G. von Schnering, R. Nesper, J. Curda, K. F. Tebbe, *Angew. Chem. Int. Ed.* **1980**, *19*, 1033–1034.

[13] I. Todorov, S. C. Sevov, *Inorg. Chem.* **2004**, *43*, 6490–6494.

[14] I. Todorov, S. C. Sevov, *Inorg. Chem.* **2005**, *44*, 5361–5369.

[15] a) N. Perez-Peralta, M. Contreras, W. Tiznado, J. Stewart, K. J. Donald, G. Merino, *Phys. Chem. Chem. Phys.* **2011**, *13*, 12975–12980; b) M. Contreras, E. Osorio, F. Ferraro, G. Puga, K. J. Donald, J. G. Harrison, G. Merino, W. Tiznado, *Chem. Eur. J.* **2013**, *19*, 2305–2310.

[16] O. Yañez, V. Garcia, J. Garza, W. Orellana, A. Vásquez-Espinal, W. Tiznado, *Chem. Eur. J.* **2019**, *25*, 2467–2471.

[17] a) T. J. Katz, *J. Am. Chem. Soc.* **1960**, *82*, 3784–3785; b) J. J. Bahl, R. B. Bates, W. A. Beavers, C. R. Launer, *J. Am. Chem. Soc.* **1977**, *99*, 6126–6127; c) P. V. R. Schleyer, D. Wilhelm, T. Clark, *J. Organomet. Chem.* **1985**, *281*, c17–c20; d) J. T. Miller, C. W. Dekock, *J. Organomet. Chem.* **1981**, *216*, 39–48; e) S. T. Liddle, *Coord. Chem. Rev.* **2015**, *293*, 211–227; f) M. Diefenbach, H. Schwarz, *Chem. Eur. J.* **2005**, *11*, 3058–3063; g) S. Mondal, J. L. Cabellos, S. Pan, E. Osorio, J. J. Torres-Vega, W. Tiznado, A. Restrepo, G. Merino, *Phys. Chem. Chem. Phys.* **2016**, *18*, 11909–11918.

[18] T. A. Keith, TK Gristmill Software, Overland Park KS, USA **2019**.

[19] C. Adamo, V. Barone, *J. Chem. Phys.* **1999**, *110*, 6158–6170.

[20] a) S. Grimme, J. Antony, S. Ehrlich, H. Krieg, *J. Chem. Phys.* **2010**, *132*, 154104; b) S. Grimme, S. Ehrlich, L. Goerigk, *J. Comput. Chem.* **2011**, *32*, 1456–1465.

[21] a) F. Weigend, R. Ahlrichs, *Phys. Chem. Chem. Phys.* **2005**, *7*, 3297–3305; b) F. Weigend, *Phys. Chem. Chem. Phys.* **2006**, *8*, 1057–1065.

[22] a) O. Yanez, R. Báez-Grez, D. Inostroza, W. A. Rabanal-León, R. Pino-Rios, J. Garza, W. Tiznado, *J. Chem. Theory Comput.* **2018**, *15*, 1463–1475; b) O. Yañez, D. Inostroza, B. Usuga-Acevedo, A. Vásquez-Espinal, R. Pino-Rios, M. Tabilo-Sepulveda, J. Garza, J. Barroso, G. Merino, W. Tiznado, *Theor. Chem. Acc.* **2020**, *139*, 41.

[23] a) W. Küchle, M. Dolg, H. Stoll, H. Preuss, *Mol. Phys.* **1991**, *74*, 1245–1263; b) W. Küchle, M. Dolg, H. Stoll, H. Preuss, *J. Chem. Phys.* **1994**, *100*, 7535–7542; c) P. Fuentealba, H. Preuss, H. Stoll, L. Von Szentpály, *Chem. Phys. Lett.* **1982**, *89*, 418–422; d) P. Fuentealba, L. Von Szentpaly, H. Preuss, H. Stoll, *J. Phys. B* **1985**, *18*, 1287; e) A. Bergner, M. Dolg, W. Küchle, H. Stoll, H. Preuß, *Mol. Phys.* **1993**, *80*, 1431–1441.

[24] a) C. Riplinger, F. Neese, *J. Chem. Phys.* **2013**, *138*, 034106; b) C. Riplinger, B. Sandhoefer, A. Hansen, F. Neese, *J. Chem. Phys.* **2013**, *139*, 134101; c) C. Riplinger, P. Pinski, U. Becker, E. F. Valeev, F. Neese, *J. Chem. Phys.* **2016**, *144*, 024109.

[25] a) D. G. Truhlar, *Chem. Phys. Lett.* **1998**, *294*, 45–48; b) F. Neese, A. Hansen, D. G. Liakos, *J. Chem. Phys.* **2009**, *131*, 064103.

[26] P. Pyykkö, *J. Phys. Chem. A* **2015**, *119*, 2326–2337.

[27] J. M. Millam, V. r. Bakken, W. Chen, W. L. Hase, H. B. Schlegel, *J. Chem. Phys.* **1999**, *111*, 3800–3805.

[28] a) D. Y. Zubarev, A. I. Boldyrev, *Phys. Chem. Chem. Phys.* **2008**, *10*, 5207–5217; b) D. Y. Zubarev, A. I. Boldyrev, *J. Org. Chem.* **2008**, *73*, 9251–9258.
[29] K. B. Wiberg, *Tetrahedron* **1968**, *24*, 1083–1096.
[30] a) A. D. Becke, K. E. Edgecombe, *J. Chem. Phys.* **1990**, *92*, 5397–5403; b) T. Lu, F.-W. Chen, *Acta Phys. Chim. Sin.* **2011**, *27*, 2786–2792.
[31] a) J. Jusélius, D. Sundholm, J. Gauss, *J. Chem. Phys.* **2004**, *121*, 3952–3963; b) H. Fliegl, S. Taubert, O. Lehtonen, D. Sundholm, *Phys. Chem. Chem. Phys.* **2011**, *13*, 20500–20518.

Manuscript received: November 22, 2023
Accepted manuscript online: December 12, 2023
Version of record online: December 27, 2023